Electronic Supplementary Material (ESI) for Journal of Materials Chemistry B.

Supplementary Information:

Exceptional Stability of Ultrasmall Cubic Copper Metal Nanocluster - A Molecular Dynamics Study

Nayana Edavan Chathoth[†a*], Hafila Khairun
S[†a], Manya Krishna[b], and Padmesh Anjukandi[a*]
[a]*Department of Chemistry,*
Indian Institute of Technology Palakkad,
Palakkad, 678623, Kerala, India.
[b]*Department of Chemistry,*
National Institute of Technology Meghalaya,
Shillong, ,793003, Meghalaya, India.
[†]*Contributed Equally.*

I. SIMULATION METHOD

The coinage MNCs (Cu, Ag, and Au) of cubic morphologies with different sizes (N) composed of 14, 63, 108, 172, 256, 365, 500, 666, 864 and 1099 number of atoms each were built using VESTA (Visualization for Electronic and Structural Analysis) software[1]. In each case, the initial structure was taken as perfect fcc cubic MNCs (Fig. 1). The edge lengths of each MNCs containing different number of atoms were plotted and these were identified to be in the nanoclusters regime as indicated in Fig. 1 in the main manuscript. The MNCs containing atoms N = 14, 63, 108, and 172 were identified to have dimensions less than 1.5 nm, thus classifying themselves to ultrasmall MNCs. To incorporate the IL in the simulation, 1-butyl-1,1,1-trimethylammonium methanesulfonate [N1114][C1SO3] was built using Avogadro[2] and the forcefield parameters were obtained using an Automated force field Topology Builder (ATB)[3]. The Heinz group's Lennard-Jones parameters for MNCs were considered which was used to maintain the non-bonded interactions of metals[4]. The Cu nanocluster was initially placed in the centre of the cubic simulation box of 5 nm^3 dimensions and solvation was taken care by SPC/E (simple point charge) water model[5]. Similar procedures were repeated for MNCs of Ag and Au. In the case of the MNCs in IL, 300 molecules (ion pairs) of the [N1114][C1SO3] IL were placed around the nanocluster within the MNC-water system of 5 nm^3 simulation box so as to maintain a concentration of 4 M[6]. Thus MNCs and MNC-IL systems were obtained prior to MD run for all systems. MD simulations were carried out for 100 ns using GROMACS (Groningen Machine for Chemical Simulations) 2020.1 version[6] with the parameterized GROMOS 53a6 force field[7] being utilized for all of the MNCs and MNC-IL simulations.

The energy minimization for 50000 steps was done using the steepest descent method. The equilibration of energy minimized systems at constant volume and temperature (NVT) for 2 ns at 300 K was done using the velocity-rescale thermostat[9], followed by a 2 ns equilibration at constant pressure and temperature (NPT) with fixed pressure of 1 bar using Parrinello−Rahman barostat[10]. The final MD runs were carried out using leap frog integrator for 100 ns. The time steps chosen was 2 fs. The output trajectory was printed for every 0.002 ns. Particle Mesh Ewald method[11] maintains the long range electrostatic interactions. LINCS algorithm accounts for all bond constraints[12]. Periodic boundary conditions were taken in xyz directions. The trajectories of the simulation were clustered prior to any analysis and GROMACS utilities were employed to analyze the root Mean Square deviation (RMSD), Solvent Accessible Surface Area (SASA), and radial distribution function (RDF) of the NCs in both water and 4 M IL-water mixture. Visualization of the molecular structures were performed using VMD 1.9.3[8].

II. SUPPLEMENTARY FIGURES

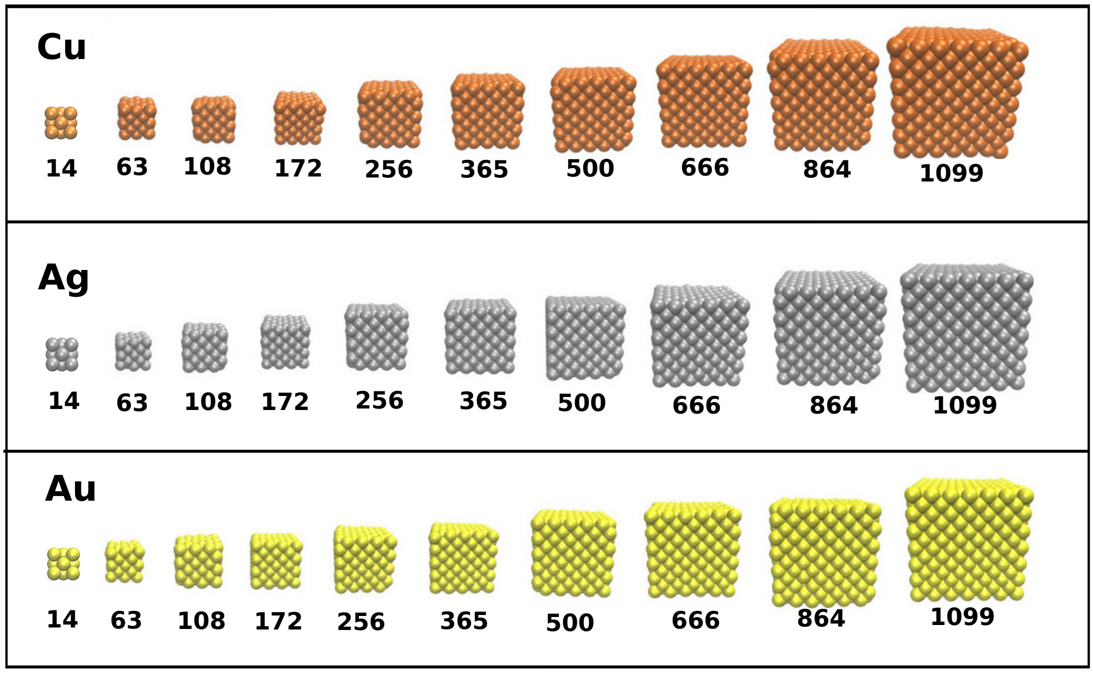

FIG. S1: Schematic representation of the various size (Number of atoms, N) dependent cubic nanoclusters (NC) of Cu, Ag, and Au metals respectively.

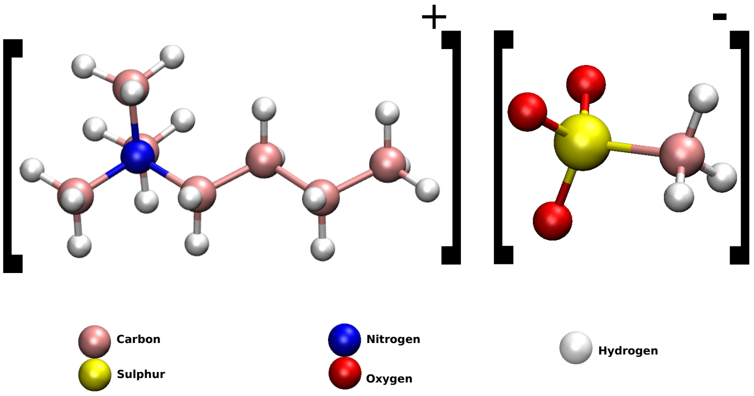

FIG. S2: Schematic representation of 1-butyl-1,1,1-trimethyl ammonium methane sulfonate ([N1114][C1SO3]) ionic liquid.

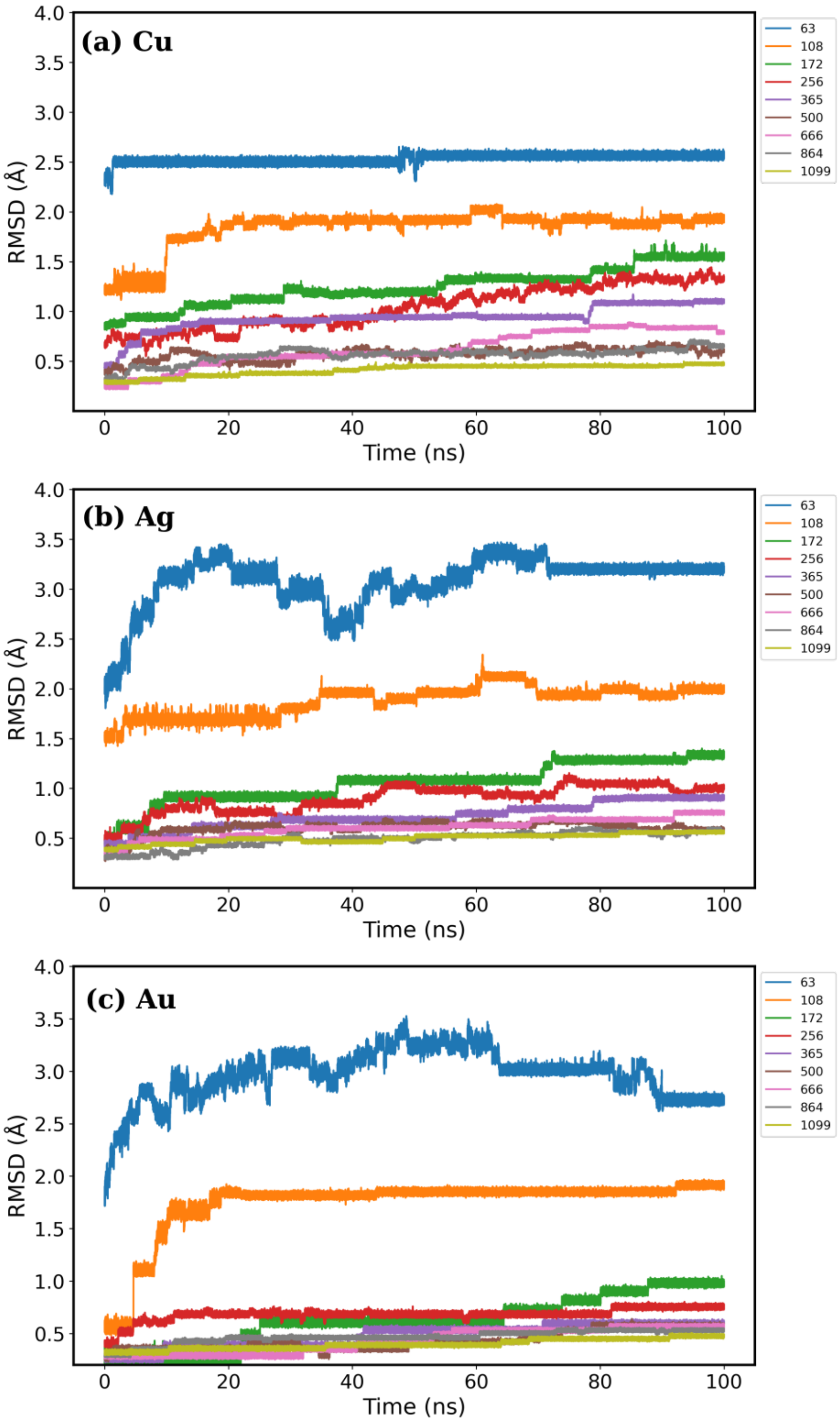

FIG. S3: The time evolution of the root mean square deviation (RMSD) for different size nanoclusters of size ranging from N = 63 to 1099 for (a) Cu, (b) Ag, and (c) Au over a simulation trajectory of 100 ns in water, starting form the perfect cubic geometry. It can be clearly seen that smaller NCs (N < 256) deviate from the starting geometry readily compared to the bigger geometries that deviates to a lesser extent.

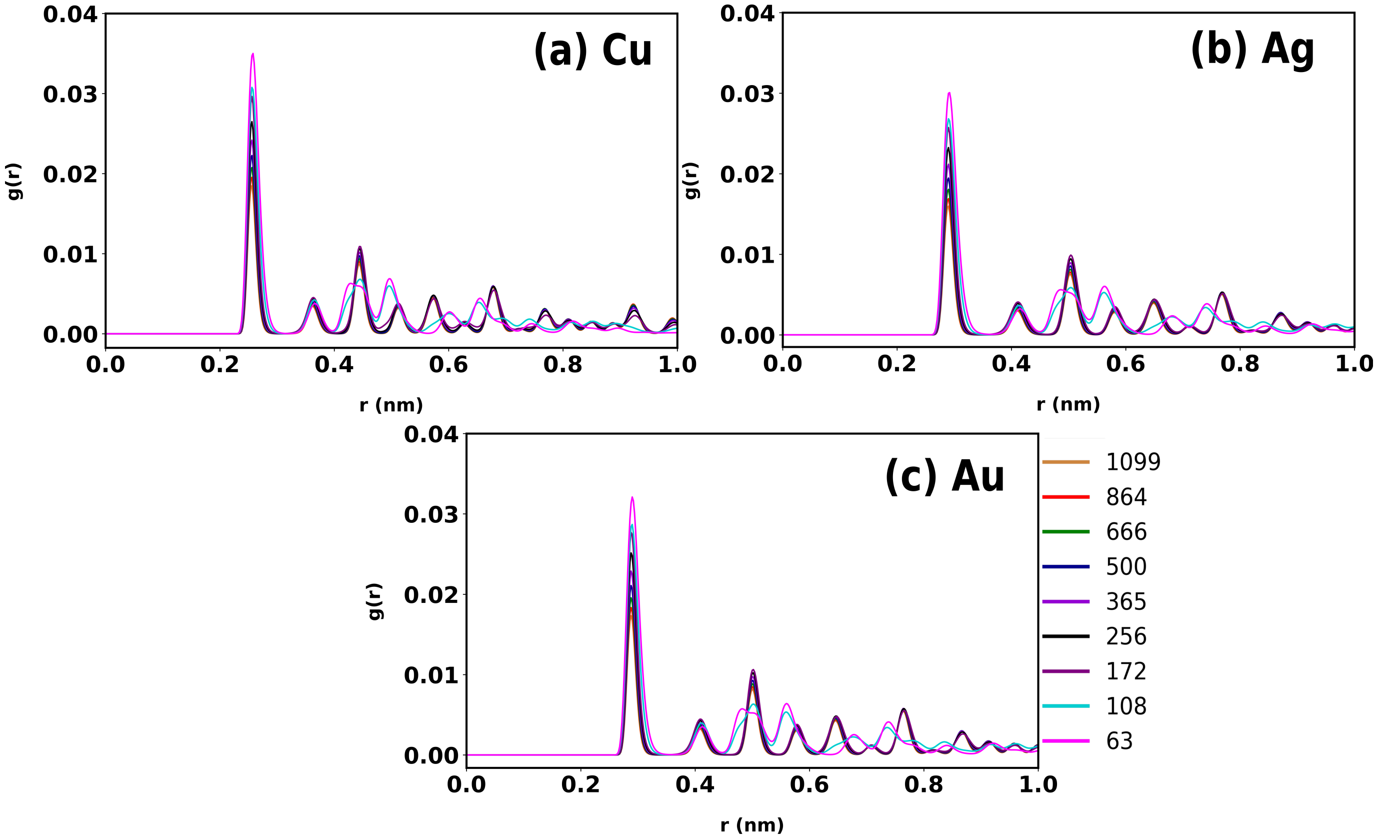

FIG. S4: Normalized radial distribution function, g(r) for the metal to metal distance for (a) Cu, (b) Ag, and (c) Au in bulk water. Data was truncated at r=1 nm due to the presence of a flat curve, which does not provide any meaningful information regarding the radial distribution function (RDF) of the system.

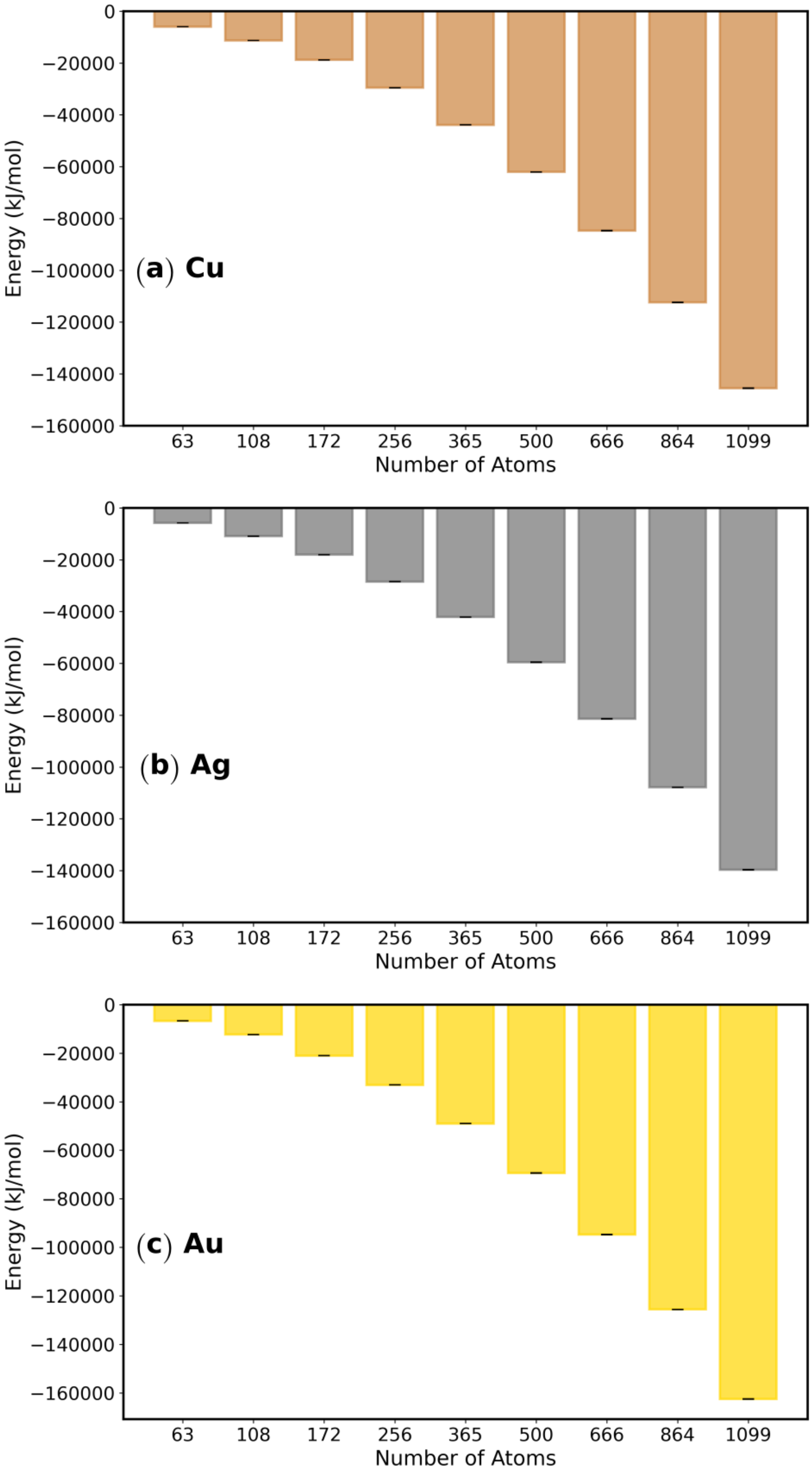

FIG. S5: Non-bonded short range van der Waals interaction energies between the metal atoms of (a) Cu, (b) Ag, and (c) Au respectively in presence of water.

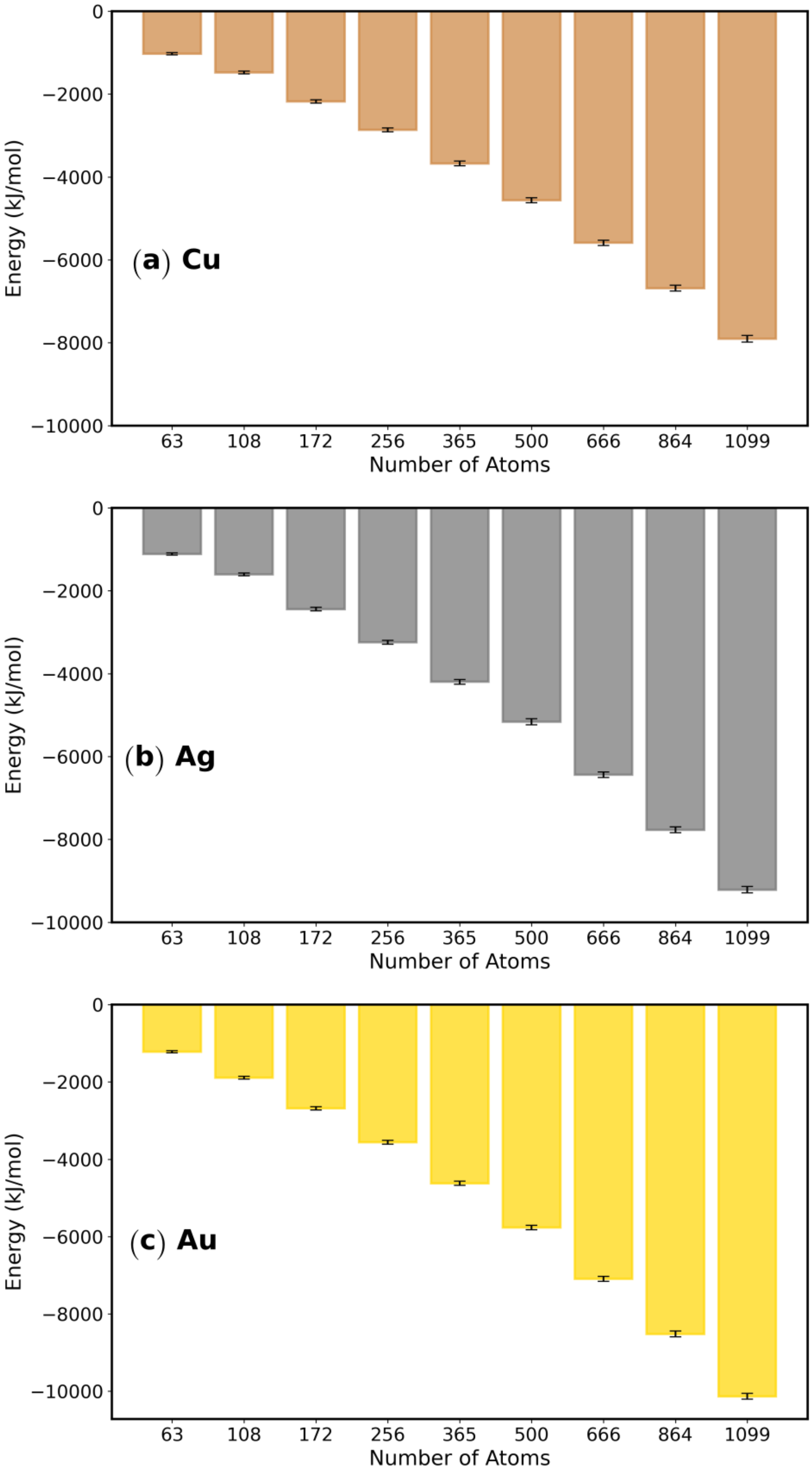

FIG. S6: Non-bonded short range van der Waals interaction energies between the metal atoms of (a) Cu, (b) Ag, and (c) Au metals respectively with that of the water.

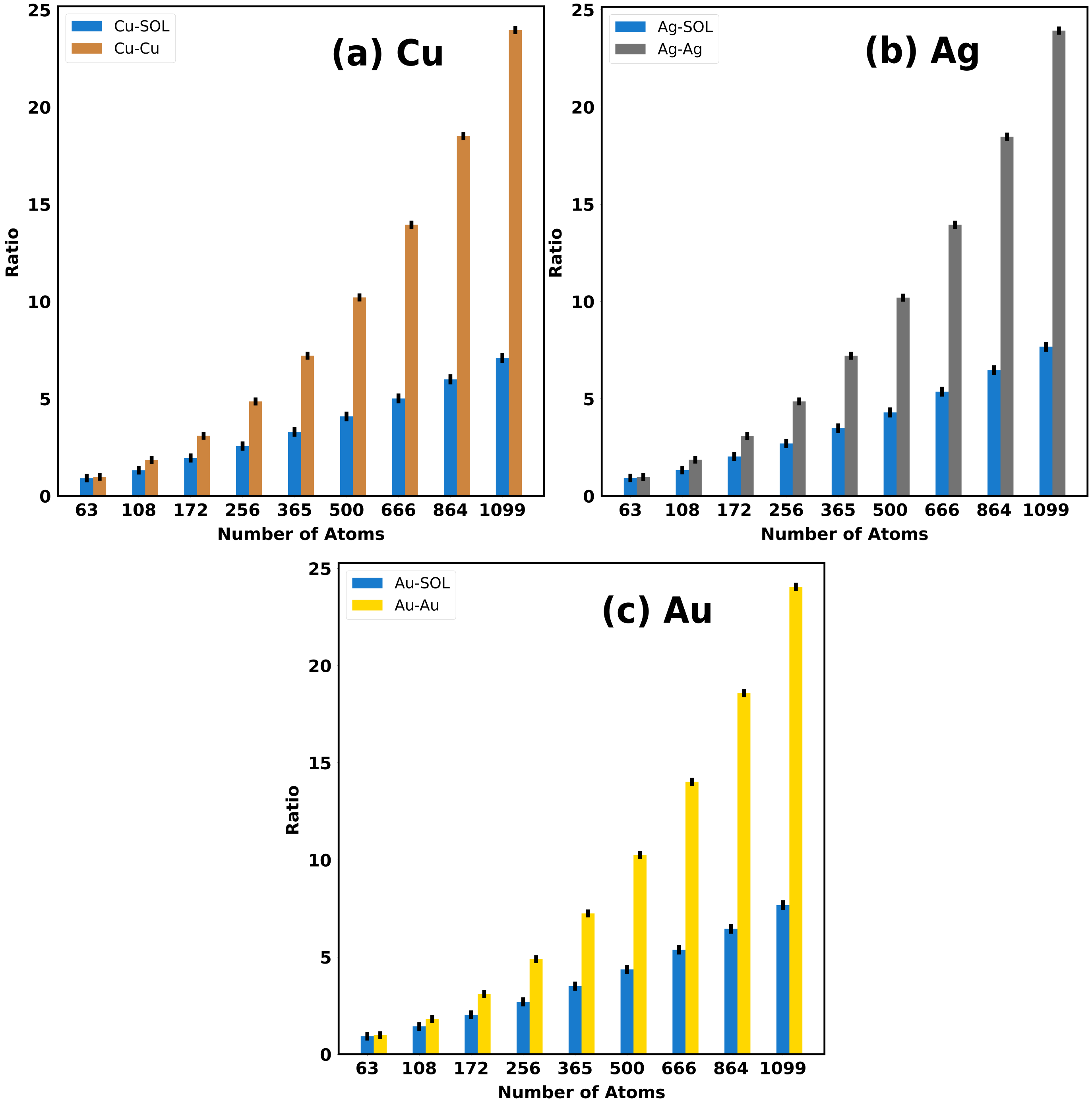

FIG. S7: The comparison of the Non-bonded short range van der Waals interaction energies between M-M and M-SOL of (a) Cu, (b) Ag, and (c) Au [M=Metal, SOL=water]. The ratio was taken by dividing the energies of each N by the lowest energy (corresponding to N=63)

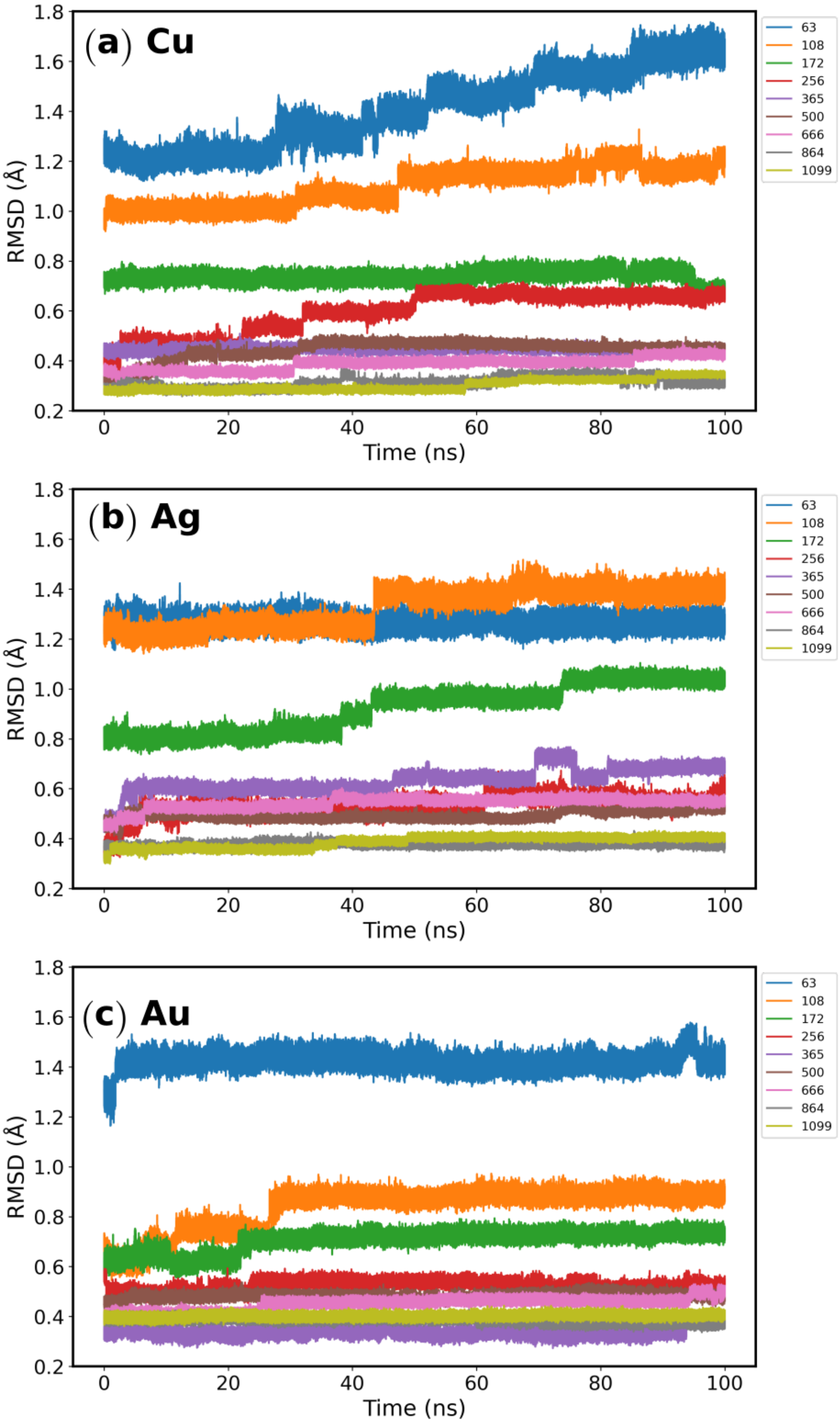

FIG. S8: The time evolution of the root mean square deviation (RMSD) for different size nanoclusters of size ranging from N = 63 to 1099 over a simulation trajectory of 100 ns in 4 M IL-water mixture, starting form the perfect cubic geometry. It can be clearly seen that in presence of the IL, the NCs attain comparative size stability.

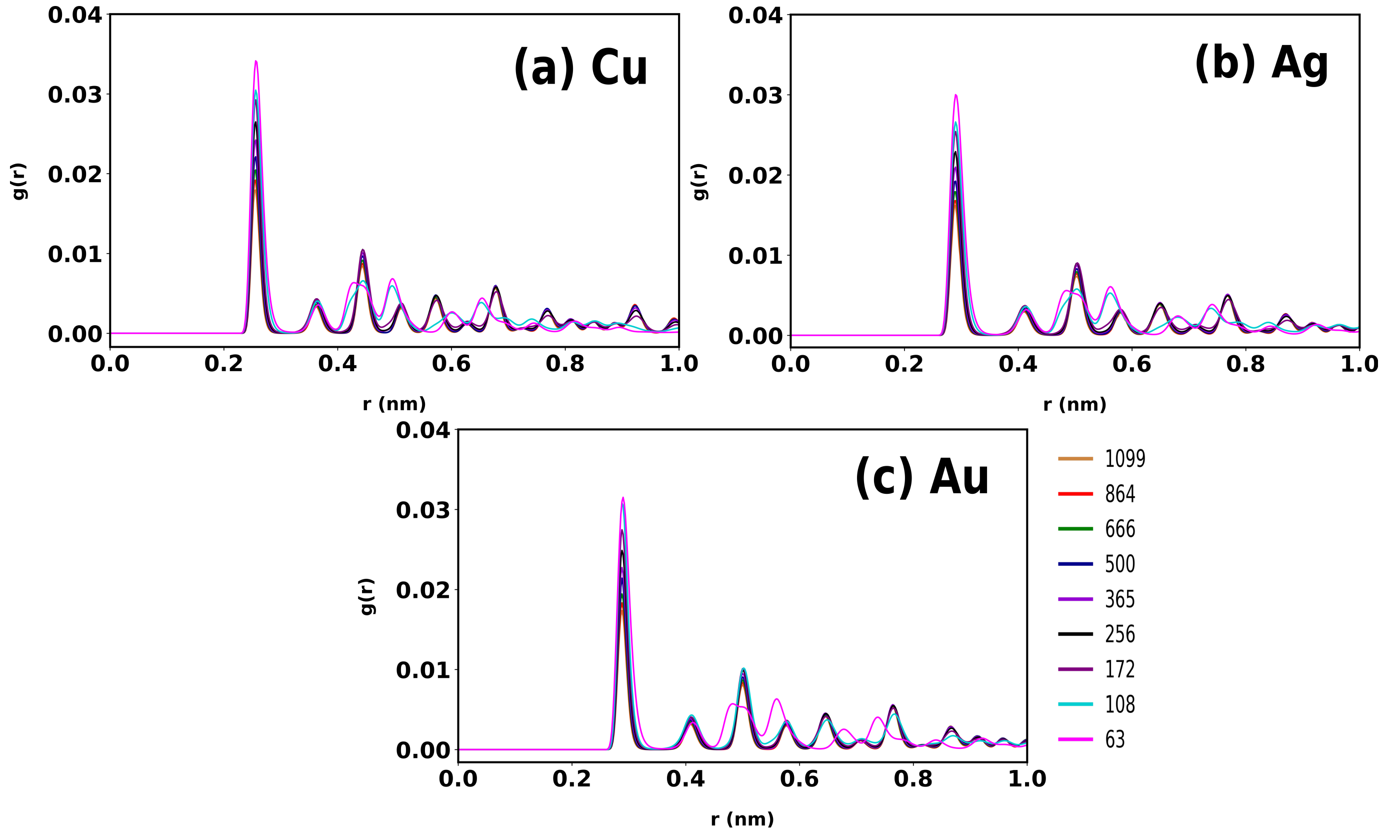

FIG. S9: Normalized radial distribution function , g(r) for the metal to metal distance for (a)Cu, (b) Ag, and (c) Au in 4 M IL-water mixture. Data was truncated at r=1 nm due to the presence of a flat curve, which does not provide any meaningful information regarding the radial distribution function (RDF) of the system.

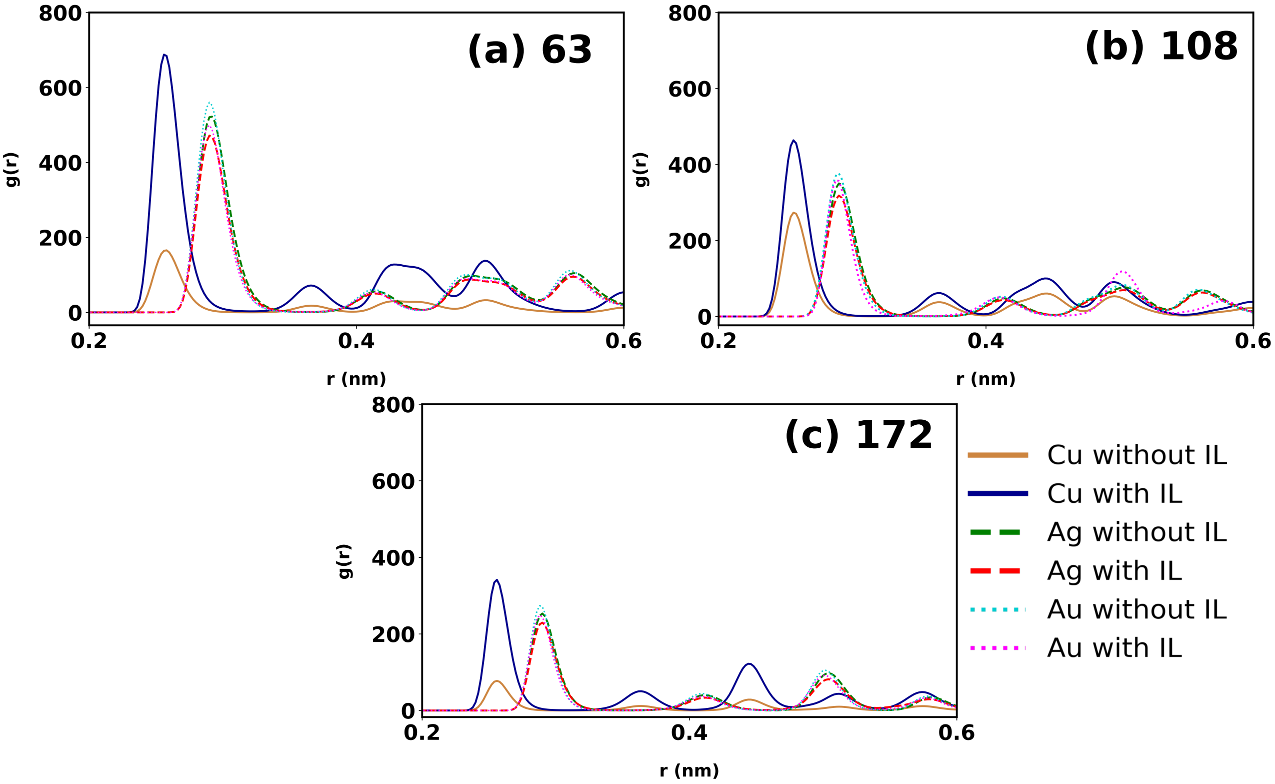

FIG. S10: Radial distribution function, g(r) for the metal to metal distance for MNC with size (a) 63, (b) 108 and (c) 172 in the presence and absence of IL. Data was truncated at r=0.6 nm as they do not provide any meaningful information regarding the radial distribution function (RDF) of the system.

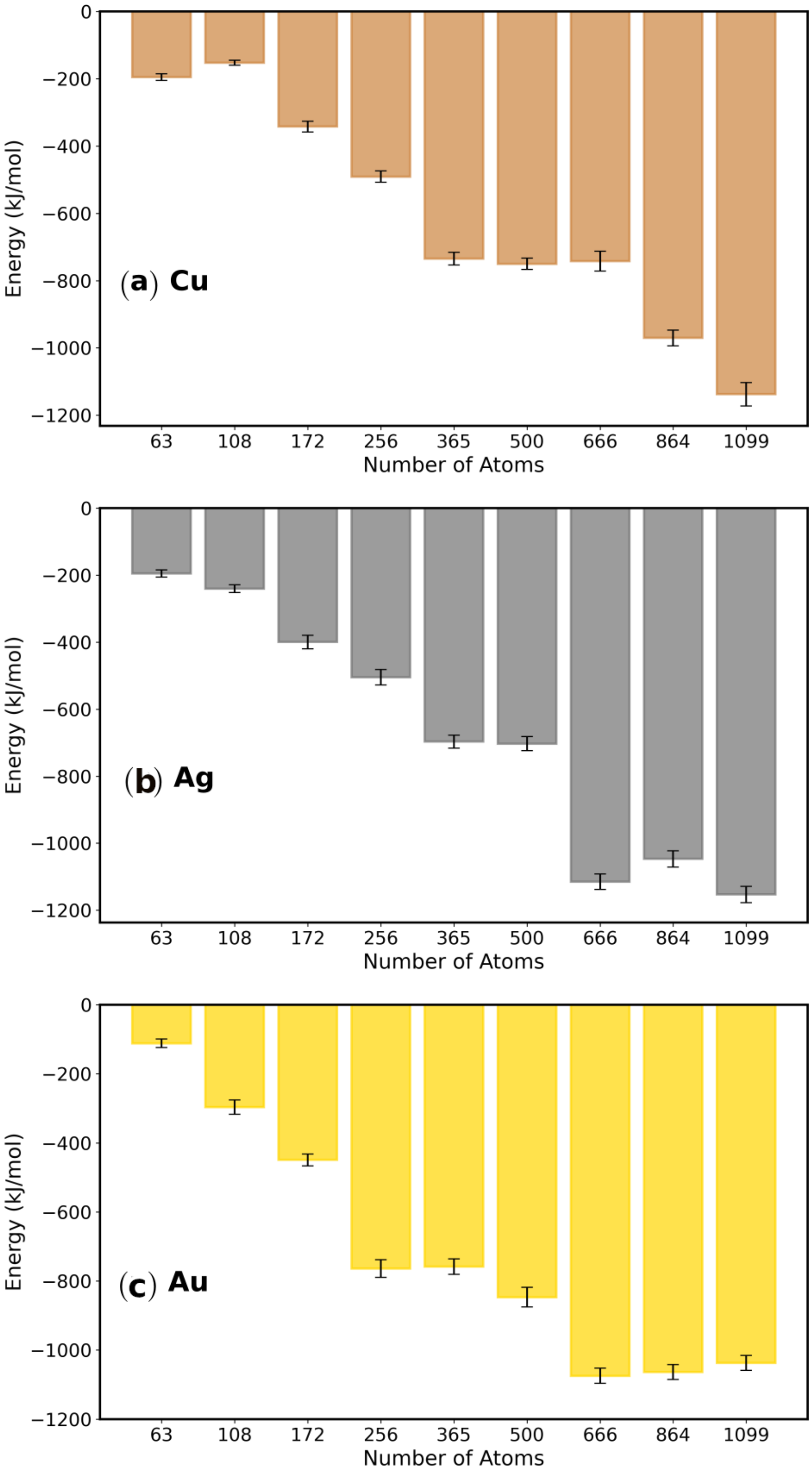

FIG. S11: Non-bonded short range van der Waals interaction energies between the metal atoms of (a) Cu, (b) Ag, and (c) Au metals respectively and the water solvent in presence of 4 M IL-water solution.

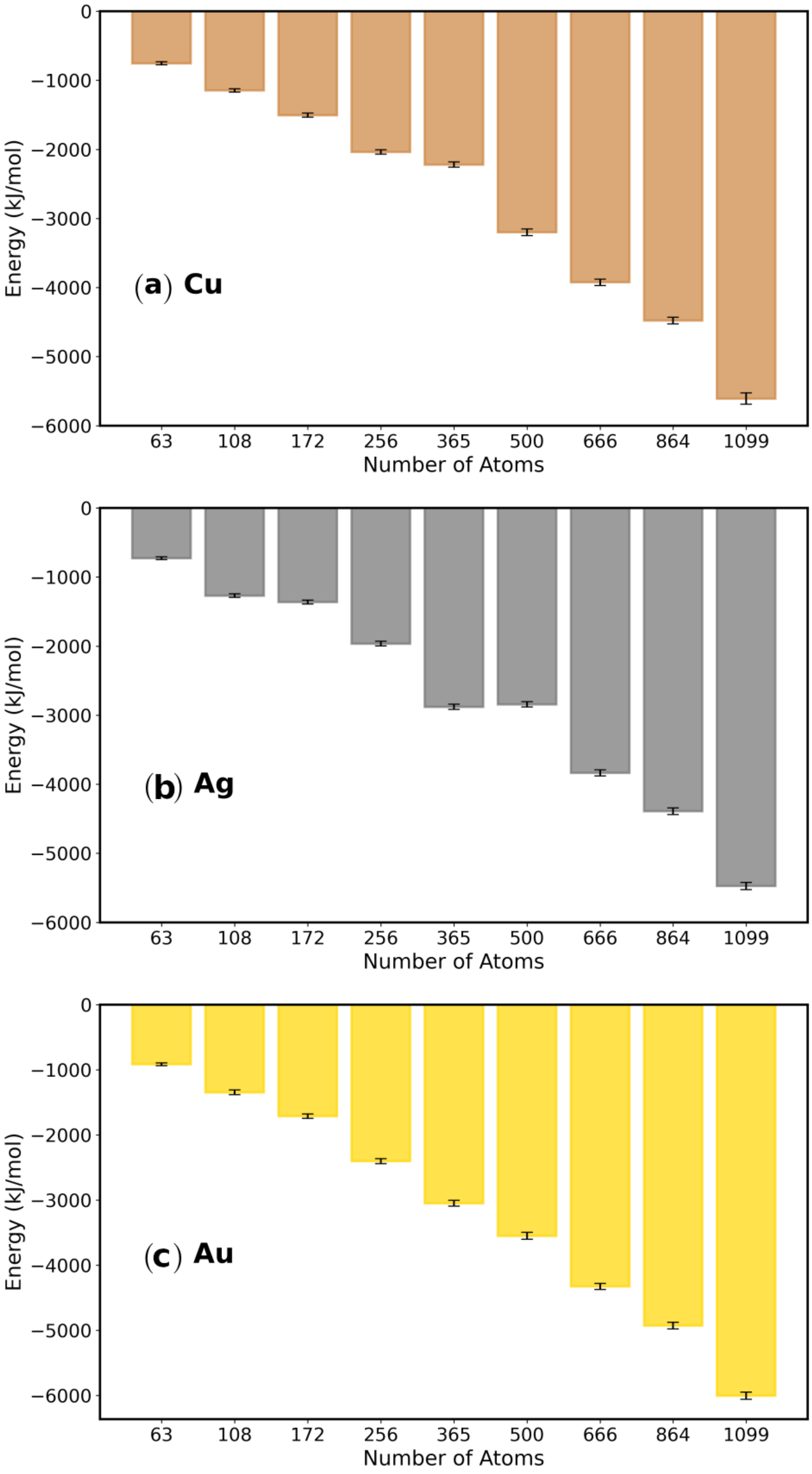

FIG. S12: Non-bonded short range van der Waals interaction energies between the metal atoms of (a) Cu, (b) Ag, and (c) Au metals respectively and the negatively charged ions ($C1SO_3$) of the IL in presence of 4 M IL-water solution.

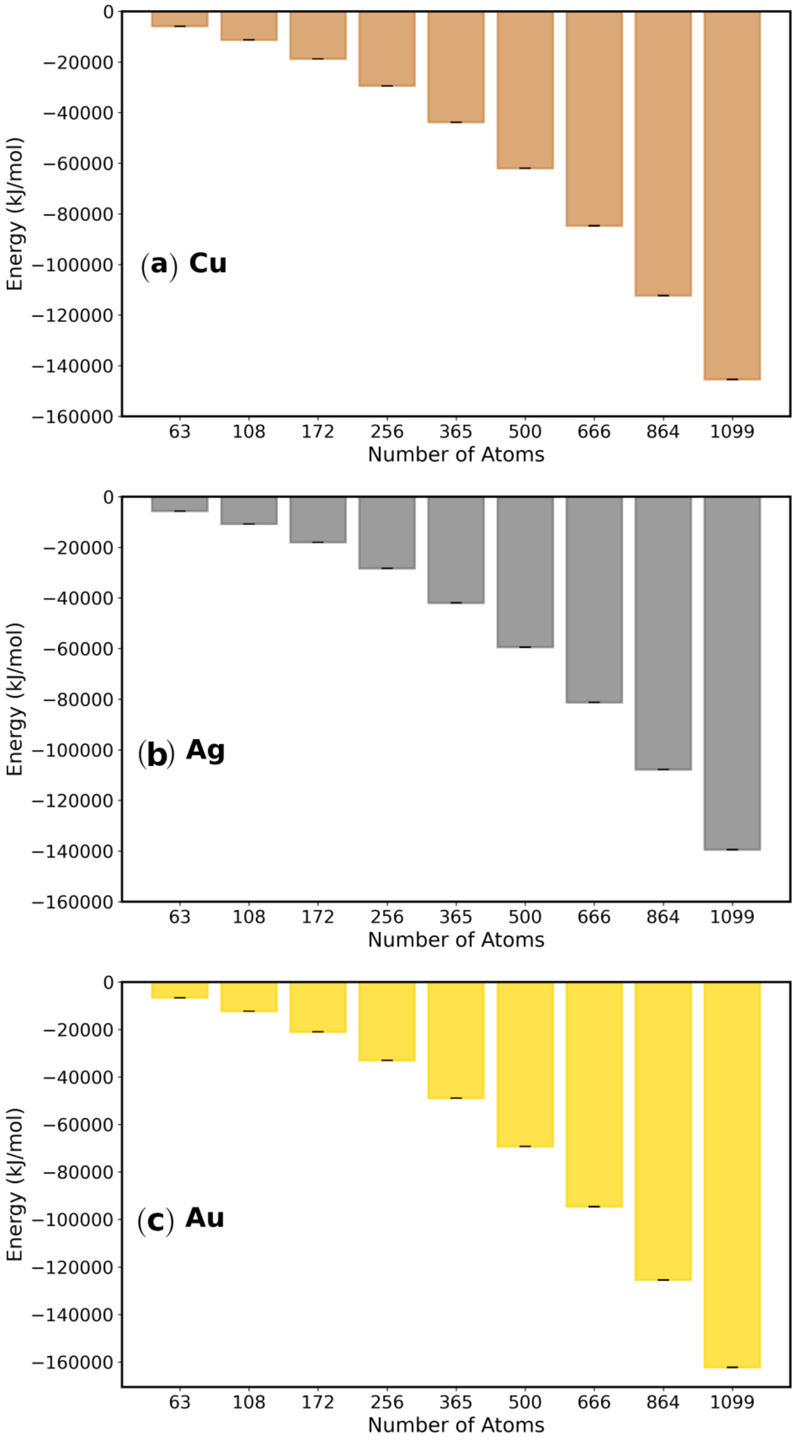

FIG. S13: Non-bonded short range van der Waals interaction energies between the metal atoms of (a) Cu, (b) Ag, and (c) Au metals respectively in presence of 4 M IL-water solution.

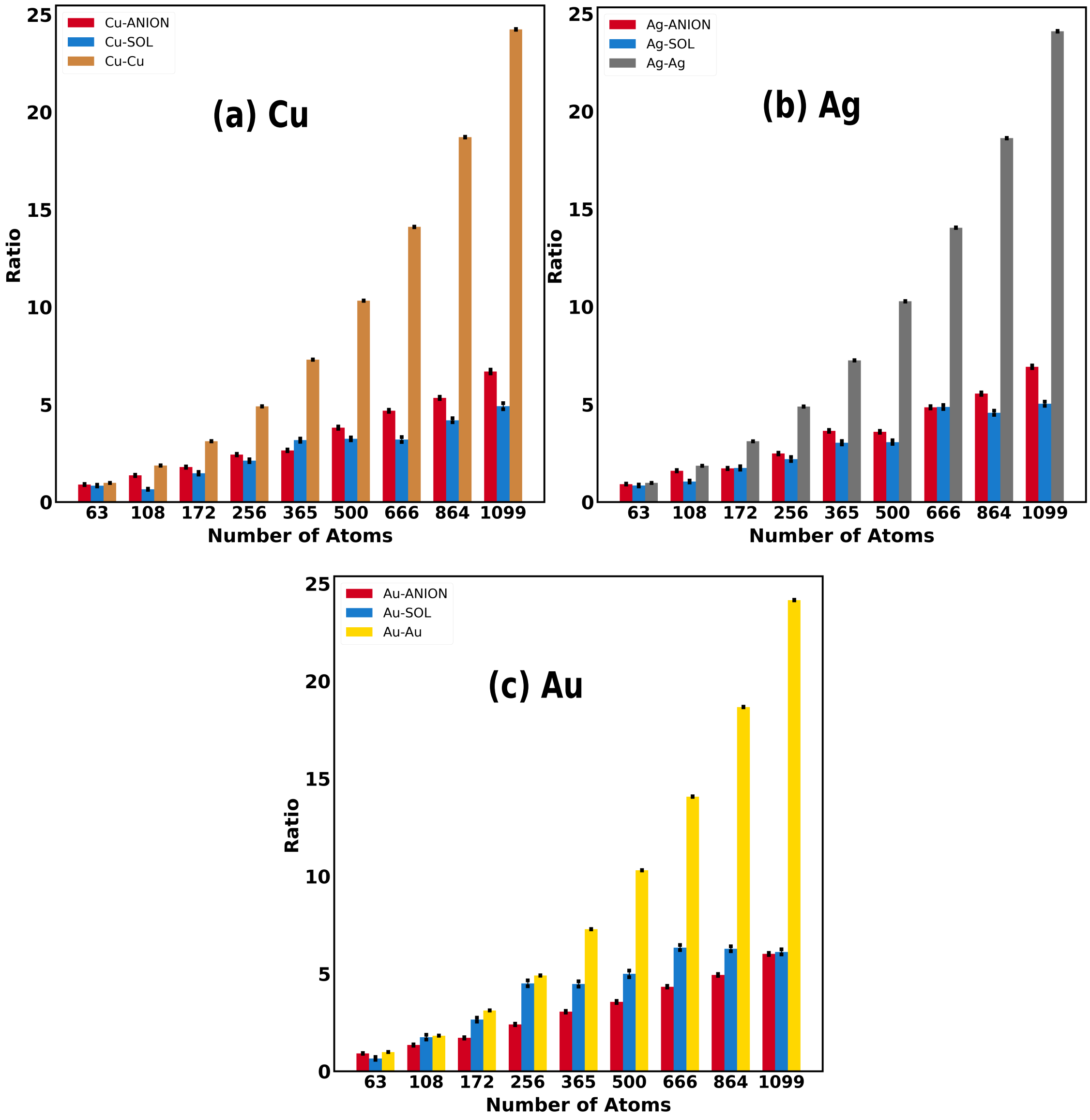

FIG. S14: The comparison of the non-bonded short range van der Waals interaction energies between M-M, M-SOL and M-ANION of (a) Cu, (b) Ag, and (c) Au [M=Metal, SOL=water, ANION= Anion of the IL] in 4 M IL-water mixture. The ratio was taken by dividing the energies of each N by the lowest energy (corresponding to N=63)

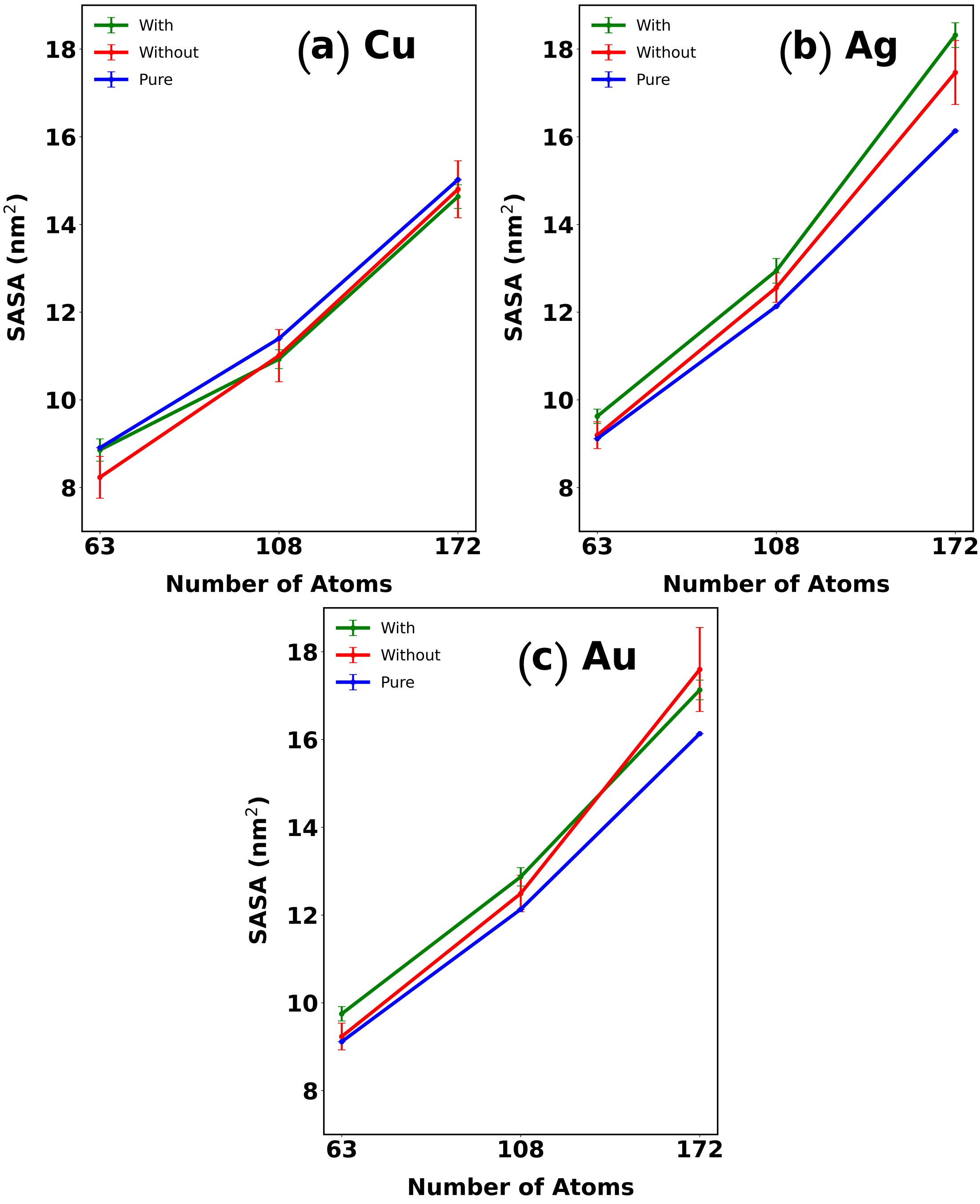

FIG. S15: The calculated SASA for different metal NCs at the sizes N=63 to 172. The blue curve denotes the SASA of the perfect cubic shaped starting structures of the respective cubic NCs. The red and the green curves denotes the time averaged SASA for the respective cubic NCs over the 100 ns trajectory without and with IL. At these sizes of the MNCs, it can be observed that the Cu MNC exhibits no difference when it comes to the SASA in pure form or with or without IL. While in the case of Ag and Au, without and with IL simulations exhibits considerable deviation in SASA even at these length scales.

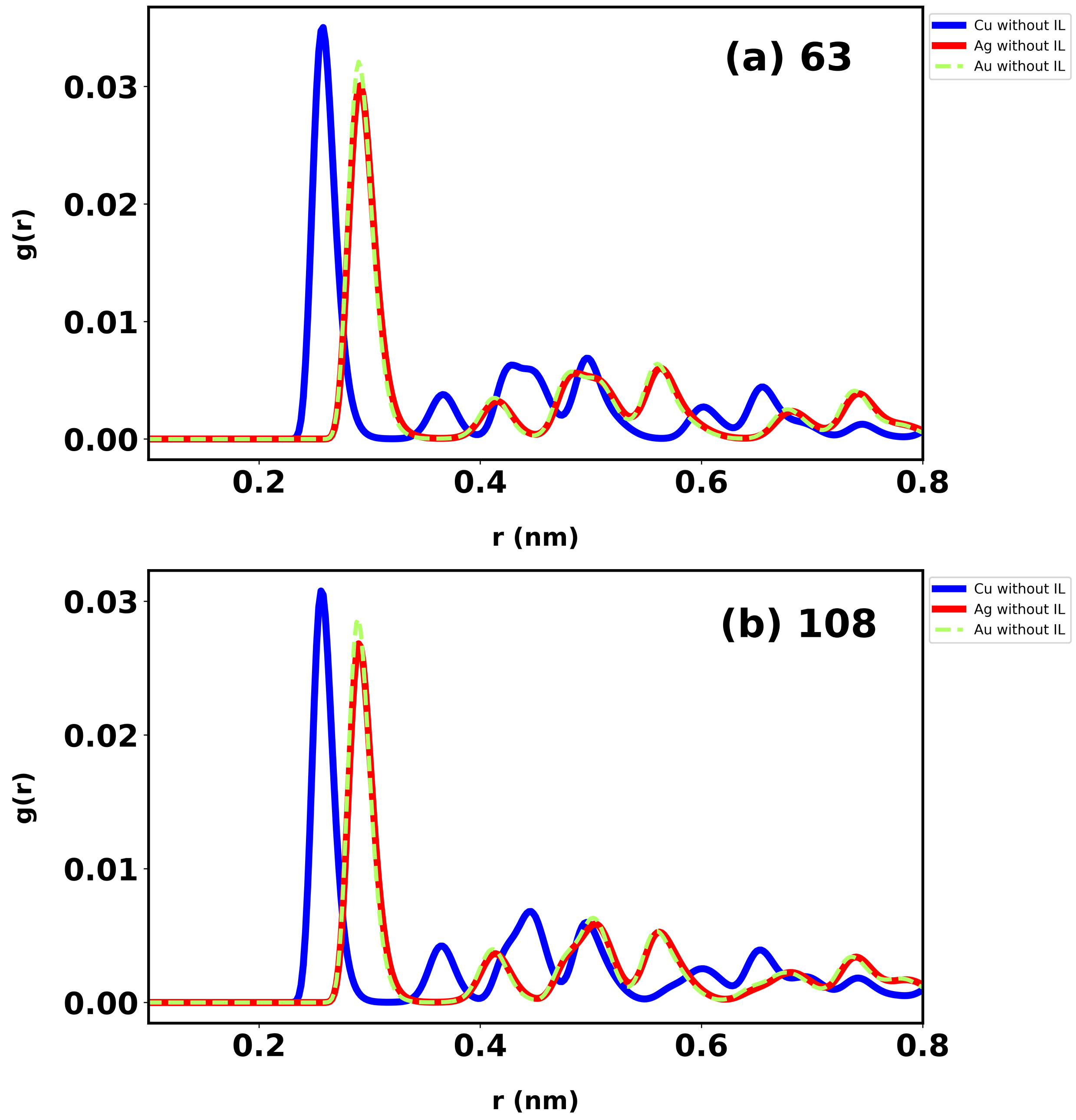

FIG. S16: Normalized radial distribution function, g(r) for the metal to metal distance for Cu, Ag, and Au MNCs with size of (a) 63 and (b) 108 in the absence of IL. Data was truncated at r=0.8 nm after which they do not provide any meaningful information regarding the radial distribution function (RDF) of the system

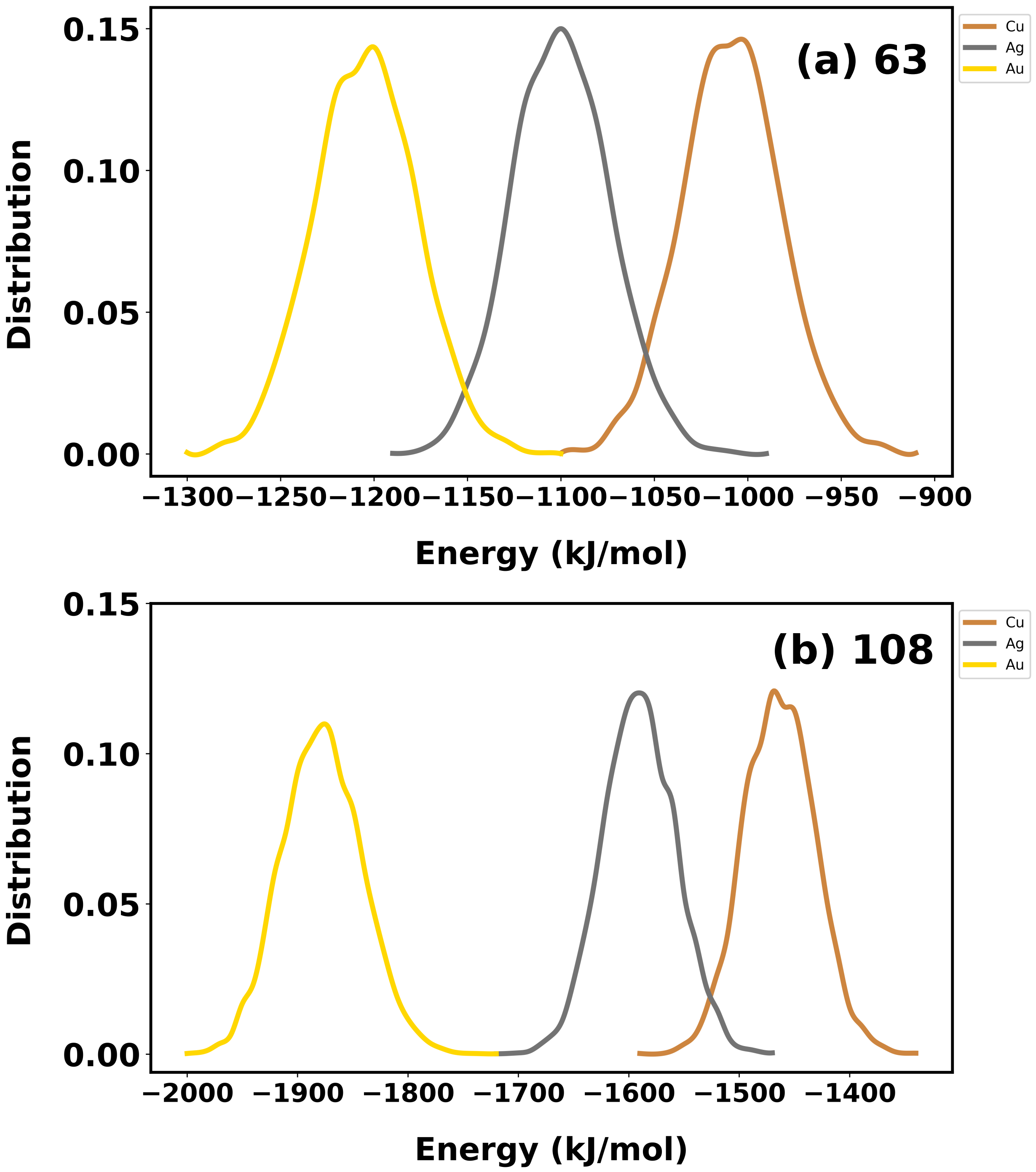

FIG. S17: Distribution of non-bonded short range van der Waals interaction energies between the metal atoms of Cu, Ag, and Au with the water molecules, with number of atoms of each MNC being (a) N=63 and (b) N=108.

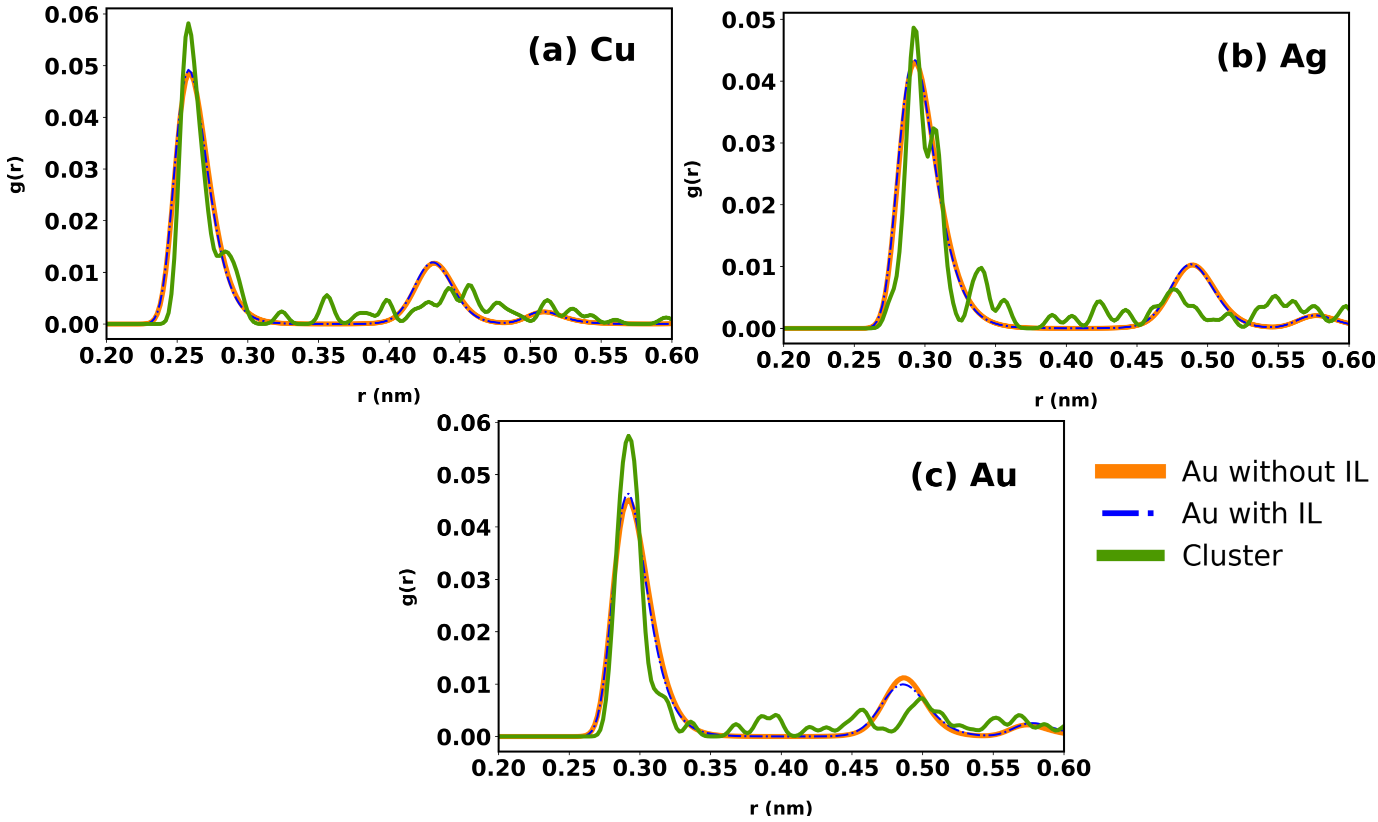

FIG. S18: The RDF plots for M-M for (a) Cu, (b) Ag, and (c) Au in the crystal structure, in the presence of IL and in the absence of IL.

	RMSD(Å)	SASA(nm^2)	E_{M-M}(kJ/mol)	E_{M-SOL}(kJ/mol)
Cu	2.008±0.29	3.91±0.18	-894.50±11.68	-329.48±13.46
Ag	2.632±0.16	3.98±0.10	-861.93±11.90	-363.58±14.26
Au	2.089±0.25	3.95±0.11	-1007.64±11.58	-395.56±14.72

TABLE I: RMSD, SASA and interaction energies of MNCs with size N=14 in bulk water

	RMSD(Å)	SASA(nm^2)	E_{M-M}(kJ/mol)	E_{M-SOL}(kJ/mol)	$E_{M-ANION}$(kJ/mol)
Cu	1.163±0.15	3.92±0.17	-857.90±11.32	-41.63± 6.03	-284.31±12.52
Ag	1.68±0.04	3.95± 0.10	-862.62±11.89	-38.00±5.09	-324.89±12.26
Au	1.15±0.03	4.05± 0.08	-958.85±13.85	41.18±6.26	-346.43±15.77

TABLE II: RMSD, SASA and interaction energies of MNCs with size N=14 in 4 M IL-water mixture

---

[*] Electronic address: `padmesh@iitpkd.ac.in,201914002@smail.iitpkd.ac.in`

[1] K. Momma and F. Izumi, *J. Appl. Cryst.*, 2011, **44**, 1272–1276.

[2] M. D. Hanwell, D. E. Curtis, D. C. Lonie, T. Vandermeersch, E. Zurek and G. R. Hutchison, *Journal of cheminformatics*, 2012, **4**, 1–17.

[3] A. K. Malde, L. Zuo, M. Breeze, M. Stroet, D. Poger, P. C. Nair, C. Oostenbrink and A. E. Mark, *J. Chem. Theory and Comput.*, 2011, **7**, 4026–4037.

[4] H. Heinz, R. Vaia, B. Farmer and R. Naik, *J. Phys. Chem. C*, 2008, **112**, 17281–17290.

[5] H. J. C. Berendsen, J. R. Grigera and T. P. Straatsma, *The Journal of Physical Chemistry*, 1987, **91**, 6269–6271.

[6] M. N. Jorabchi, M. Abbaspour, E. K. Goharshadi and S. Wohlrab, *J. Mol. Liquids*, 2022, **360**, 119447.

[7] C. Oostenbrink, A. Villa, A. E. Mark and W. F. Van Gunsteren, *J. Comp. Chem.*, 2004, **25**, 1656–1676.

[8] W. Humphrey, A. Dalke and K. Schulten, *Journal of molecular graphics*, 1996, **14**, 33–38.

[9] G. Bussi, D. Donadio and M. Parrinello, *J. Chem. Phys.*, 2007, **126**, 014101.

[10] M. Parrinello and A. Rahman, *J. Appl. Phys*, 1981, **52**, 7182–7190.

[11] T. Darden, D. York and L. Pedersen, *The Journal of Chemical Physics*, 1993, **98**, 10089–10092.

[12] Z. Hazarika and A. N. Jha, *ACS omega*, 2019, **5**, 170–178.